NASA TECHNICAL NOTE

NASA TN D-6600

THE ESTIMATION OF GALACTIC COSMIC RAY PENETRATION AND DOSE RATES

by M. O. Burrell and J. J. Wright

George C. Marshall Space Flight Center
Marshall Space Flight Center, Ala. 35812

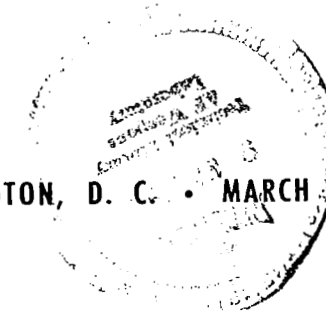

NATIONAL AERONAUTICS AND SPACE ADMINISTRATION • WASHINGTON, D. C. • MARCH 1972

1. Report No.	2. Government Accession No.	3. Recipient's Catalog No.
NASA TN D-6600		

4. Title and Subtitle	5. Report Date
The Estimation of Galactic Cosmic Ray Penetration and Dose Rates	March 1972
	6. Performing Organization Code
7. Author(s)	8. Performing Organization Report No.
M. O. Burrell and J. J. Wright	M444
	10. Work Unit No.
9. Performing Organization Name and Address	
George C. Marshall Space Flight Center Marshall Space Flight Center, Alabama 35812	11. Contract or Grant No.
	13. Type of Report and Period Covered
12. Sponsoring Agency Name and Address	Technical Note
National Aeronautics and Space Administration Washington, D. C. 20546	14. Sponsoring Agency Code

15. Supplementary Notes

Prepared by Space Sciences Laboratory

16. Abstract

This study is concerned with approximation methods that can be readily applied to estimate the absorbed dose rate from cosmic rays in rads – tissue or rems inside simple geometries of aluminum. The present work is limited to finding the dose rate at the center of spherical shells or behind plane slabs. The dose rate is calculated at tissue-point detectors or for thin layers of tissue. This study considers cosmic-ray dose rates for both free-space and earth-orbiting missions.

17. Key Words (Suggested by Author(s))	18. Distribution Statement

19. Security Classif. (of this report)	20. Security Classif. (of this page)	21. No. of Pages	22. Price*
Unclassified	Unclassified	45	$3.00

*For sale by the National Technical Information Service, Springfield, Virginia 22151

TABLE OF CONTENTS

		Page
SECTION I.	INTRODUCTION	1
SECTION II.	PRIMARY PROTON PENETRATION METHODS	1
SECTION III.	METHODS FOR HEAVY NUCLEI	7
SECTION IV.	RELATIVE ABUNDANCE AND ENERGY SPECTRA OF COSMIC RAYS	13
SECTION V.	FREE SPACE COSMIC RAY DOSE ANALYSIS	16
SECTION VI.	CALCULATION OF COSMIC RAY DOSE RATES FOR EARTH ORBITAL MISSIONS	25
SECTION VII.	CONCLUSIONS	35
REFERENCES		39

LIST OF ILLUSTRATIONS

Figure	Title	Page
1.	Delayed effect quality factor as a function of average LET	4
2.	Proton stopping power in tissue as a function of energy	6
3.	Geometry effects of primary particles and secondaries in a spherical shell geometry	11
4.	Differential spectra of free space hydrogen and helium nuclei during solar minimum	16
5.	Cosmic-ray dose rates in rads as a function of shield thickness	21
6.	Cosmic-ray dose rates in rems as a function of shield thickness	26
7.	Cosmic-ray dose rates in rems for very heavy nuclei	26
8.	Comparison of cosmic ray dose rates as a function of shield thickness	27
9.	Differential energy spectra for protons in a 463-km orbit	30
10.	Differential energy spectra for helium nuclei in a 463-km orbit	30
11.	Cosmic-ray dose rates in rads in a 463-km orbit as a function of orbit inclination and shield thickness	32
12.	Cosmic-ray dose rates in rems in a 463-km orbit as a function of orbit inclination and shield thickness	32
13.	Cosmic-ray dose rates in rads as a function of orbit altitude and inclination	36
14.	Cosmic-ray dose rates in rems as a function of orbit altitude and inclination	36
15.	Cosmic-ray dose rates in rads as a function of orbit altitude for two inclinations	37

LIST OF TABLES

Table	Title	Page
1.	Values of QF for Late or Delayed Effects as a Function of Average LET	3
2.	Range Constants for $R_p = \frac{a}{2b} \ln (1 + 2b E^r)$	5
3.	Relative Abundances of Cosmic Ray Nuclei Outside Earth's Magnetic Field	12
4.	Differential Spectra of Hydrogen and Helium $\frac{\text{particles}}{\text{cm}^2\text{-sec-MeV/nucleon}}$	15
5.	Values of Inelastic Cross Section in Al^{27}	19
6.	Summary of Calculated Cosmic Ray Doses in Rads-Tissue/Year Normalized to 4 particles/cm^2-sec Above 30 MeV/nucleon	20
7.	Dose Estimated by Relative Abundancies Times Z^2 Dependence	22
8.	Summary of Calculated Cosmic Ray Doses in rem/year Normalized to 4 particles/cm^2-sec Above 30 MeV/nucleon	23
9.	Cosmic Ray Dose Rates from V.G. Bobkov et al. [2.3 particles/cm^2-sec]	24
10.	Nuclei Groups for Orbital Calculations	31
11.	Summary of Cosmic Ray Pseudo-Total Doses in rads/tissue/year for 463-km Circular Orbits	33
12.	Summary of Cosmic Ray Pseudo-Total Doses in rem/year for 463-km Circular Orbits	34
13.	Summary of Cosmic Ray Pseudo-Total Dose Rates Behind 1 g/cm^2 Shield for Circular Orbits at High Altitudes	38

THE ESTIMATION OF GALACTIC COSMIC RAY PENETRATION AND DOSE RATES

SECTION I. INTRODUCTION

This study is concerned with approximation methods that can be readily applied to estimate the absorbed dose rate from cosmic rays in rads-tissue or rems inside simple geometries of aluminum. The present work will be limited to finding the dose rate at the center of spherical shells or behind plane slabs. The dose rate will be calculated at tissue-point detectors or for thin layers of tissue. To estimate tissue depth dose, a tissue thickness of 5 cm is approximated fairly well by using 6.5 g/cm^2 (2.41 cm) of an aluminum-equivalent shield. This study will consider cosmic-ray dose rates for both free-space and earth-orbiting missions.

SECTION II. PRIMARY PROTON PENETRATION METHODS

The foundation of the present work will be the straight-ahead, or one-dimensional approximation used by the author to calculate proton penetration and dose rates [1,2]. As a brief summary of these methods it is assumed that the range of protons in a given material from about 10 MeV[1] to about 2000 MeV can be well approximated by a functional curve fit given by

$$R = F(E) \quad [g/cm^2] \tag{1}$$

Now as the proton penetrates the shield, the relationship between the shield depth x and the energy is given by

$$R - x = F(E - \Delta E) \quad , \tag{2}$$

where ΔE is the energy loss and $x = \Delta R$ is the change in range. Now if $E - \Delta E$ is replaced by E^* and called the energy at depth x in the shield, then it is found that

$$F(E) = x + F(E^*) \tag{3}$$

---

1. To convert electron volts to SI units (joules), multiply by 1.60210×10^{-19}.

or

$$E = g_x(E^*) = F^{-1}\,[x + F(E^*)]$$

Now if a differential energy spectrum is given by

$$\phi(E)\ [\text{proton/cm}^2 - \text{MeV-sec}]\ ,\ E_1 \leqslant E \leqslant E_2 \quad ,$$

then the primary proton differential spectrum at depth x is given by

$$\phi_x(E^*) = e^{-\Sigma_{in} x}\,\phi_o\left\{ g_x(E^*)\right\} \left|\frac{dg_x(E^*)}{dE^*}\right| \quad ;\ E_1^* \leqslant E^* \leqslant E_2^* \quad , \tag{4}$$

where $E_1^* = g_x^{-1}(E_1)$; $E_2^* = g_x^{-1}(E_2)$ and Σ_{in} is the inelastic cross section. The inelastic cross section is assumed to be constant for our purpose; see References 1 and 2 for justification. Now the primary proton absorbed dose rate in rads-tissue can be calculated as simply

$$D_p(x) = 1.6 \times 10^{-8} \int_{E_1^* \geqslant 0}^{E_2^*} \phi_x(E^*)\, S_o(E^*)\, dE^* \left[\frac{\text{rads-tissue}}{\text{sec}}\right] \quad , \tag{5}$$

where $S_o(E)$ is the proton stopping power in tissue. If one wishes to find the equivalent dose in rems, the equation becomes simply

$$D_p(x) = 1.6 \times 10^{-8} \int_{E_2^* \geqslant 0}^{E_2^*} \phi_x(E^*)\, QF(E^*)\, S_o(E^*)\, dE^* \left[\frac{\text{rems}}{\text{sec}}\right] \quad , \tag{6}$$

where QF(E*) is the quality factor for late effects as a function of E* (in the shield). The quality factor for late or delayed effects is used since the anticipated dose rates are expected to be less than 0.1 rad-tissue/day from cosmic rays.

Now the quality factor is measured by the linear energy transfer or LET in keV/μm in tissue or water. Since water and tissue are very close in LET values, the relationship between L(keV/μm) and S_o(MeV - cm^2/g) is

$$\bar{L} \cong \frac{S_o(E)}{10} \left[\frac{keV}{\mu m}\right] , \tag{7}$$

where $S_o(E^*)$ is the proton-stopping power in tissue. Now, from Reference 3, the following table is given:

TABLE 1. VALUES OF QF FOR LATE OR DELAYED EFFECTS AS A FUNCTION OF AVERAGE LET

$\bar{L}$ (LET)	QF
$\leqslant 3.5$	1.00
3.5 - 7	1 - 2
7 - 23	2 - 5
23 - 53	5 - 10
53 - 175	10 - 20
> 175	20

Because of the unknown characteristics of high LET, it will be assumed that a maximum QF of 20 is given for $\bar{L} > 175$ keV/μm. See Reference 3 for additional discussion. Figure 1 depicts the plot of the end values of Table 1. A frequently given formula for this table is $QF = 0.8 + 0.16\,\bar{L}$. This is shown as a straight line in Figure 1. However, in this work it was felt that a more accurate representation of Table 1 could be given with a minimum of computation effort; thus, the author has chosen the following formulation:

$$QF = 0.78 + 0.174\,\bar{L} , \quad \bar{L} \leqslant 53 \tag{8}$$

$$QF = 5.65 + 0.082\,\bar{L} , \quad 53 < \bar{L} \leqslant 175 \tag{9}$$

$$QF = 20 , \quad \bar{L} > 175 \tag{10}$$

For purposes intended in the present work, an approximation to the proton range in matter can be represented by

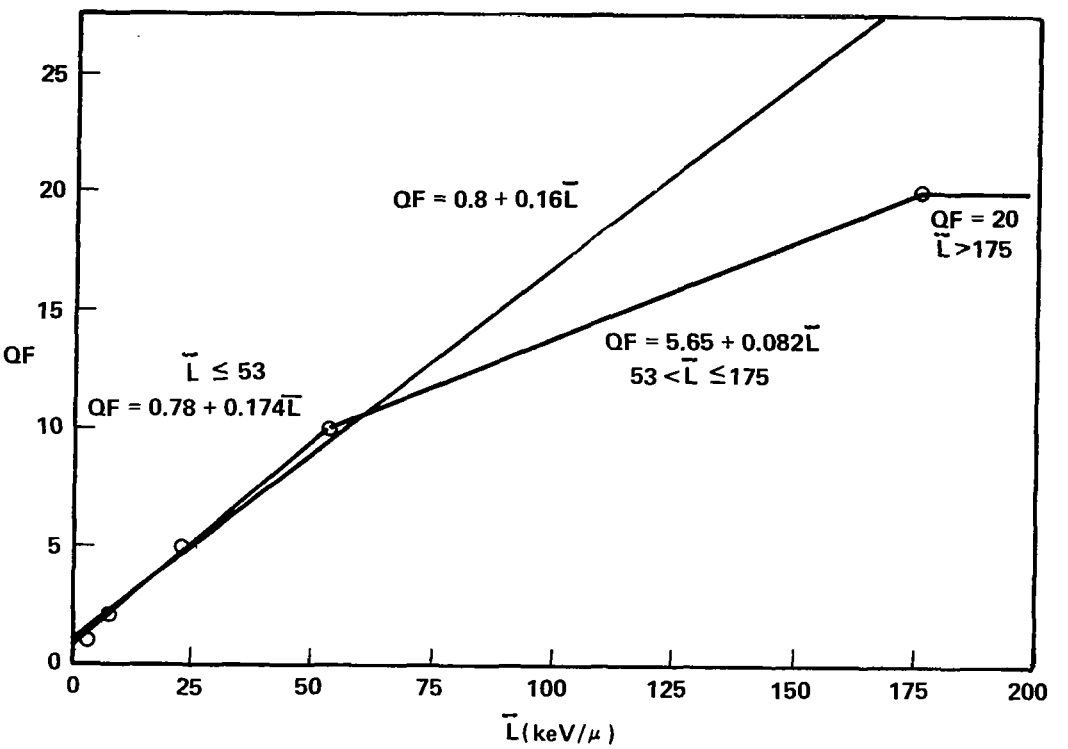

Figure 1. Delayed effect quality factor as a function of average LET.

$$R_p(E) = \frac{a}{2b} \ln (1 + 2b\, E^r) \left[\frac{g}{cm^2}\right] \quad . \tag{11}$$

where the constants a, b, and r depend on the shield materials. Table 2 provides a set of values [4] which should be adequate to verify or extend the following work.

The form of equation (11) was chosen to carry out the manipulations suggested in equations (3) through (5). Based on the definitions for proton range, it is seen that the proton-stopping power is simply given by

$$S_p(E) = \frac{1}{\frac{dR}{dE}} \quad . \tag{12}$$

TABLE 2. RANGE CONSTANTS FOR $R_p = \frac{a}{2b} \ln (1 + 2b E^r)$

Material	r	a × 10^3	b × 10^6
Carbon	1.800	2.1378	2.1488
Aluminum	1.775	2.7938	2.3455
Iron	1.750	3.5940	2.5203
Copper	1.750	3.7513	2.6491
Silver	1.725	4.8601	2.9411
Air	1.775	2.4634	2.0788
Poly	1.800	1.8094	2.1137
Tissue	1.800	1.9329	2.1623
Water	1.800	1.9293	2.1674
Glass	1.750	3.1482	2.1495

Thus,

$$S_o(E) = \frac{1}{a_o r_o} \left(\frac{1}{E^{r_o - 1}} + 2b_o E \right) \quad , \tag{13}$$

where a_o, b_o and r_o are chosen to give the best stopping-power fit for protons in tissue up to about 900 MeV. Beyond about 900 MeV, the stopping power is assumed to be essentially constant (Fig. 2).

Now referring to equation (3), it is seen that one needs to find the energy external to the shield in terms of the energy inside the shield. Application of equation (3) to equation (11) yields the following relationships:

$$E = g_x(E^*) = (\alpha + \beta E^{*r})^{1/r} \quad , \tag{14}$$

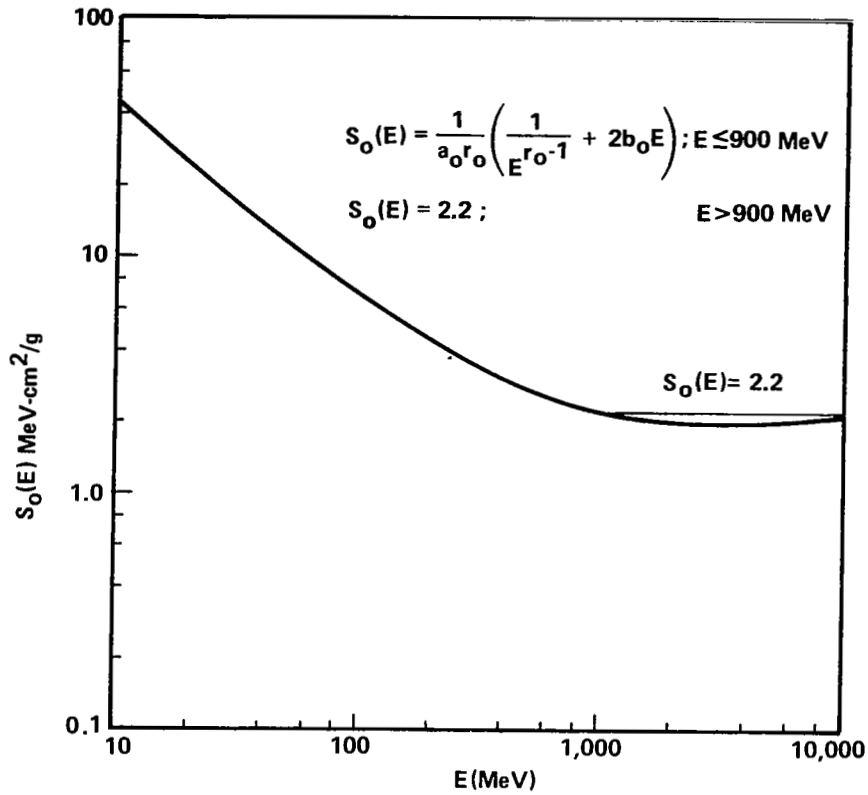

Figure 2. Proton stopping power in tissue as a function of energy.

where .

$$\beta = \exp\left(\frac{2bx}{a}\right) \text{ and } \alpha = \frac{1}{2b}(\beta - 1) \quad .$$

From equation (14), it follows that

$$E^* = \left(\frac{E^r - \alpha}{\beta}\right)^{1/r} \quad \text{if} \quad E > \alpha^{1/r} \tag{15}$$

$$E^* = 0 \quad \text{if} \quad E \leqslant \alpha^{1/r} \quad .$$

At this point the author wishes to diverge from the methods of References 1 and 2 and also from equations (4) and (5) of this report. Since the cosmic-ray spectra have energy units of MeV/nucleon and extend to energies of many thousands of MeV/nucleon, it was

found that the form of equations (4) and (5) led to numerical difficulties that were most readily resolved, as follows. Instead of using the spectrum at depth x, one can use the incident spectrum and still calculate the dose at depth x by using a translated stopping-power function. Thus, if one uses the stopping power that a proton will have after traversing x g/cm^2, then he can find the proper primary dose by using the incident spectrum, as follows:

$$D_p(x) = 1.6 \times 10^{-8}\, e^{-\Sigma_{in} x} \int_{E=\alpha^{1/r}}^{E_{max}} \phi_o(E)\, S_x(E^*)\, dE \quad , \tag{16}$$

where

$$S_x(E^*) = \frac{1}{a_o r_o} \left(\frac{1}{E^{*r_o - 1}} + 2 b_o E^* \right)$$

and

$$E^* = \left(\frac{E^r - \alpha}{\beta} \right)^{1/r} ; \; E > \alpha^{1/r} \quad . \tag{17}$$

Note that the constants a, b, and r are chosen for the shield, while the constants a_o, b_o, r_o are chosen for tissue-stopping power (Table 2). In like manner, one calculates the dose in rem but the $\bar{L} = S_x(E^*)/10$ (keV/μ), where the stopping power is calculated as above. The above equations are equivalent to finding the minimum energy to penetrate to a depth x ($E = \alpha^{1/r}$), discarding this lower portion of the spectrum, and then using the stopping power of the remaining energies modified to reflect the translated energies of the original spectrum. This, of course, is only valid if Σ_{in} is independent of the proton energy which is not quite true, but, for cosmic-ray transport, it is felt to be sufficient at the present level of knowledge and technique.

SECTION III. METHODS FOR HEAVY NUCLEI

The techniques discussed in the previous section were limited to protons, but the transition to heavy nuclei is based upon the validity of the methods for protons. The first modification in approach is that from this point on the units of energy will usually be in MeV/nucleon and will be designated by E_A (MeV/nucleon) = E/A. Now it is a common

assumption that for heavy, fully-charged ions with energies sufficiently high to prevent charge pickup ($E_A > 10$ MeV/nucleon), the stopping power and range for protons can be used in the following manner to estimate the stopping power and range of heavy ions:

$$S_A(E) = Z^2 \, S_p(E_A) \tag{18}$$

$$R_A(E) = \frac{A}{Z^2} \, R_p(E_A) \quad , \tag{19}$$

where A is the mass number of the incident ion and Z is the atomic number or charge. The $S_p(E_A)$ and $R_p(E_A)$ denote the proton-stopping-power and range function in a given material but with E_A (energy per nucleon) replacing the proton energy.

Now since the major purpose of the range formula [equation (19)] is to find the energy E_A^* at depth x, the following procedure is used. The proton range equation (11) is substituted as the funtional part of equation (19) and then at depth x in a shield;

$$\frac{A}{Z^2} \left[\frac{a}{2b} \ln (1 + 2b \, E_A^r)\right] = x + \frac{A}{Z^2} \left[\frac{a}{2b} \ln (1 + 2b \, E_A^{*r})\right] \quad . \tag{20}$$

See equation (3). The above can be simplified to read:

$$E_A = (\alpha_A + \beta_A \, E_A^{*r})^{1/r} \left[\frac{\text{MeV}}{\text{nucleon}}\right] \quad , \tag{21}$$

where

$$\beta_A = \exp\left(\frac{2bx}{a} \cdot \frac{Z^2}{A}\right)$$

and

$$\alpha_A = \frac{1}{2b} (\beta_A - 1) \quad ,$$

or

$$E_A^* = \left(\frac{E_A^r - \alpha_A}{\beta_A} \right)^{1/r} \quad ; \; E_A^* = 0 \text{ if } E_A^* \leq \alpha_A{}^{1/r} \quad . \tag{22}$$

The constants a, b, and r are taken from Table 2.

Since the method of equation (16) will be used to calculate the dose rate, it follows that the dose rate for heavy ions can now be determined. First, to simplify, let a particular cosmic-ray component of heavy nuclei be represented by a differential energy spectrum; $J_o(E_A)$ = [particles/cm^2-sec-MeV/nucleon]. If above some energy θ (or 900 MeV/nucleon), the tissue stopping power is a constant, then the primary particle dose in rads-tissue can be written as follows:

$$D_p(x) = 1.6 \times 10^{-8} \, e^{-\Sigma_{in} x} \left[\int_{E_A = \alpha_A{}^{1/r}}^{(\alpha_A + \beta_A \theta^r)^{1/r}} J_o(E_A) \, S_x(E^*_A) \, dE_A + 2.2 \, Z^2 \int_{(\alpha_A + \beta_A \theta^r)^{1/r}}^{\infty} J_o(E_A) \, dE_A \right] , \tag{23}$$

where

$$S_x(E_A^*) = \frac{Z^2}{a_o \, r_o} \left[\frac{1}{E_A^{*r_o - 1}} + 2 b_o \, E_A^* \right] \tag{24}$$

and

$$E_A^* = \left(\frac{E_A^r - \alpha_A}{\beta_A} \right)^{1/r} \quad . \tag{25}$$

The lower bound energy on the first integral represents the energy which becomes zero for the primary spectrum at x g/cm^2 depth, and the upper limit denotes the energy that is translated to the energy θ at which the stopping power becomes essentially constant. The stopping power in tissue from about 900 MeV/nucleon to 30,000 MeV/nucleon can be represented well by $S_o(E) = 2.2 \, Z^2$ (MeV-cm^2/g) which is shown in the second integral. The integration to infinity assumes that the particle number decreases very rapidly

above a few BeV/nucleon, so that the underestimation in $S_o(E_A)$ is offset by the integration to infinity. Also, the form of the cosmic-ray energy spectrum for high energies is usually chosen as an analytical expression which is easily integrated.

The above method is reasonable if x is not too large. Perhaps a shield thickness of up to 50 g/cm^2 can be treated in the manner described above. Of course, the major error in calculating the dose rate is not due to the primary dose, as calculated above, but is due to the secondary particle dose from fragmentation and cascades associated with the inelastic cross section Σ_{in}. This will be discussed in more detail below, but it would seem that one could approximate the secondary contribution, when the primary dose is greater than the secondary dose, by ignoring the removal process due to inelastic collisions. Thus it is proposed that for thin shields a reasonable estimate of a pseudo-total dose (in rads) from both primaries and secondaries may be found as follows:

$$D_{total}(x) = D_p(x) \exp(+\Sigma_{in} x) ; \quad x < \frac{0.7}{\Sigma_{in}} \quad . \tag{26}$$

This was found to be reasonable for solar protons in aluminum shields of 50 g/cm^2, or more, but no similar verification is available for cosmic rays. However, the high stopping power of primary heavy nuclei, where the dose is proportional to Z^2, would tend to lend some validity to the assumption, since equation (26) implies that the fragmentation particles give the same dose as the removed primaries and the heavy fragments obviously have lower Z numbers, even though they are more numerous. For example, if a primary particle of Z = 25 breaks into four particles with Z = 6 and one with Z = 7 (velocity conserved), then the sum of squares of the charge is only 157, whereas the primary particle had a charge square of 625. Of course the above heuristic argument has neglected photons, electrons, mesons, and neutrons, but the meson-stopping power is similar in magnitude to high-energy protons and only the evaporation particles of the target nucleus are likely to have a high ionization rate.

In fact, the above argument seems more plausible for the heavy nuclei than for the protons and alphas. Looking ahead a bit to the fact that the calculated proton pseudo-total dose-rate curves are very flat, leads one to suspect that the secondaries will, in fact, give a higher dose than the removed primaries, since the stopping power of the galactic cosmic-ray proton is, in general, near minimum over most of the spectrum. Consequently, each inelastic collision can give rise to several particles (protons, alphas, neutrons, and mesons) which will easily exceed the dose of the original primary proton. This was not true for solar proton spectra where the number of low-energy protons was large (only a small fraction of the protons exceeded 500 MeV). Even at depths of 10 g/cm^2, the average spectral energy may still be 50 MeV. In this special case, the primary proton's stopping power was still quite large and the secondary yield was small in number, thus making the approximation of equation (26) quite accurate for fairly thick shields.

Yet, it is probable that if accurate secondary dose rates are calculated for the proton component of cosmic rays, the total dose curve from protons will, in fact, increase in magnitude as a function of shield thickness out, perhaps, as far as 50 g/cm^2 before the curve starts decreasing. However, care must be exercised in extrapolating this effect to the important higher-Z components. The net effect of all components may result in a nearly flat dose curve out to about 50 g/cm^2.

However, the cascading effect leads to many particles and a very insecure feeling is generated as the volume source of these particles is integrated over the shield thickness. Fortunately, the cascading particle flux tends to diverge so that when one examines a point detector at the center of a thin spherical shell the number of secondaries crossing the detector will not grow excessively. The geometry effect should result in a more uniform particle flux throughout the spherical volume. Figure 3 is an attempt to depict the likely geometry effects of cosmic-ray secondaries generated in a thin-wall vehicle whose diameter is quite large compared to the wall thickness.

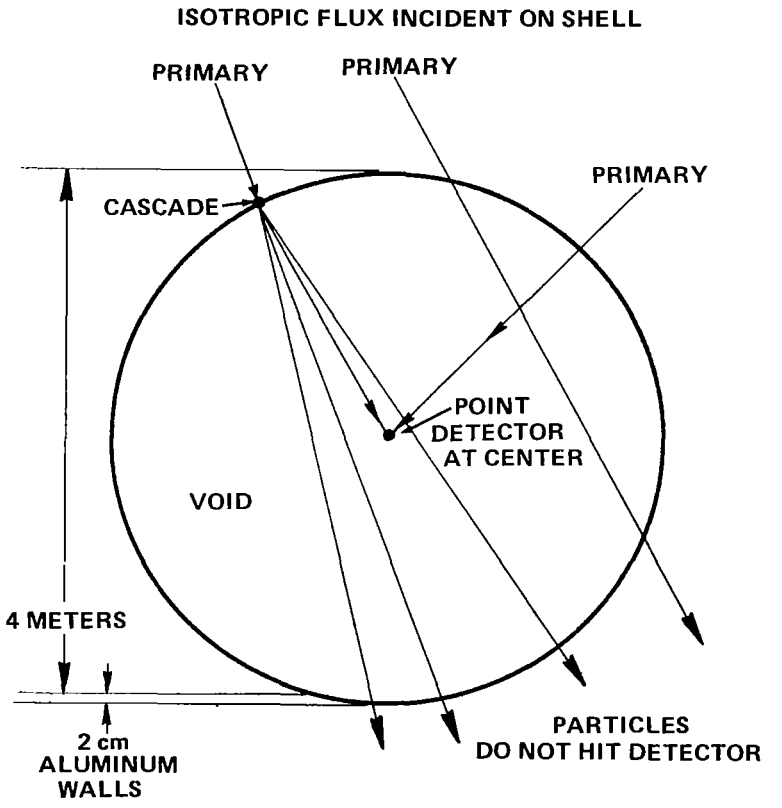

Figure 3. Geometry effects of primary particles and secondaries in a spherical shell geometry.

TABLE 3. RELATIVE ABUNDANCIES OF COSMIC RAY NUCLEI OUTSIDE EARTH'S MAGNETIC FIELD

Element	Avg Z No.	Avg A No.	Relative Abundance	f[a]
$_{1}H$	1	1	0.84700	6.2509[b]
$_{2}He$	2	4	0.13550	1.0000
$_{3}Li$-$_{5}B$	4	9	0.00311	0.0230
$_{6}C$	6	12	0.00508	0.0375
$_{7}N$	7	14	0.00226	0.0167
$_{8}O$	8	16	0.00282	0.0208
$_{9}F$	9	19	0.00028	0.0021
$_{10}Ne$	10	20	0.00085	0.0063
$_{11}Na$	11	23	0.00054	0.0040
$_{12}Mg$	12	24	0.00090	0.0066
$_{13}Al$	13	27	0.00017	0.0013
$_{14}Si$	14	28	0.00034	0.0025
$_{15}P$-$_{21}Sc$	18	37	0.00037	0.0027
$_{22}Ti$-$_{28}Ni$	25	54	0.00079	0.0058
Totals	———	———	1.00001	7.3802

a. This column is normalized to 1.000 for helium.
b. The ratio of H to He is not used for dose calculations since separate spectra are used for H and He.

SECTION IV. RELATIVE ABUNDANCE AND ENERGY SPECTRA OF COSMIC RAYS

In addition to the transport problems of secondary particles from cosmic rays, a second source of difficulty is obtaining good measurements of energy spectra of the various components of the cosmic rays. There are numerous papers and reports available with various cosmic-ray spectra and tables of relative abundances of the various cosmic-ray nuclei. However, this report will restrict itself to only one set of data in the hope that the authors' choice is representative.

The relative abundances of the various nuclei composing the cosmic-ray spectrum in this report are modified for the authors' purposes from the work of Biswas and Fichtel [5]. The results are shown in Table 3. These relative abundances vary to some degree among different writers, but the differences are not great.

In using the results of Table 3, certain assumptions will be made. The first is that for elements above hydrogen the differential energy spectrum in units of particle/(cm^2-sec-MeV/nucleon) is independent of the various species and the spectrum of a given nuclei may be found by multiplying the spectrum of helium by the ratio f of Table 3. This is not exactly true, but above about 1 GeV/nucleon this assumption is commonplace and consistent with measurements. Below 1 GeV/nucleon, the solar magnetic field and interstellar and interplanetary matter lead to a maximum point on the differential energy spectrum between about 200 and 800 MeV/nucleon, depending on the period in the solar cycle. This peak occurs at lower energies during solar minimum when the cosmic-ray flux is at a maximum in the earth's vicinity.

Following a paper by A. N. and T. N. Charakhchyan [6], the following comments are pertinent. For heavy nuclei, $A/Z \cong 2$, the magnetic rigidity of the particles in energy per nucleon will not depend on the Z number. This implies that, except for protons on a MeV/nucleon basis, the differential spectrum for all heavy nuclei ($Z \geq 2$) should look about the same except for particle absorption and energy loss by interstellar and interplanetary matter, which, however, does vary with Z number. Since this matter amounts to only a few g/cm^2, one should be on reasonably safe grounds if he assumes that the spectrum between 0.1 and 1 GeV/nucleon can be approximated by the same empirical curve shape, if $A/Z \cong 2$. For protons below 1 GeV, the differential spectrum will have a different maximum ($A/Z = 1$) and the rigidity is less at the same energy per nucleon than for a heavy particle ($Z \geqslant 2$). Based on the above work [6], the heavy nuclei differential energy spectra peaks out at about a factor of two lower than for protons. Thus, if, at solar minimum the proton differential spectra has a maximum at about 400 MeV, then the heavy ions ($A/Z \cong 2$) would have a maximum at about 200 MeV/nucleon. These assumptions seem to give fair agreement with measurements, as shown in the above article.

For the purposes of this report, it will simply be assumed that the solar cycle is at a minimum, and the total cosmic ray flux above about 30 MeV/nucleon is 4 part/cm^2-sec with 84.7 percent being protons, 13.55 percent being helium and 1.75 percent consisting of nuclei with $Z > 2$. The total flux is possibly a little high, since measurements indicate a total flux somewhat less at solar minimum. However, this number is often given as the likely maximum flux in the earth's vicinity and it will be used to scale the various spectra used in this report. It should be noted that the spectra used in the following work gives an integral flux above about 1 GeV/nucleon of about 1.95 particle/cm^2-sec.

For energies above about 1 GeV/nucleon, the galactic cosmic-ray differential energy spectra is usually depicted by an equation of the form:

$$J_o(E_A) = \frac{fN}{(M_o + E_A)^{2.5}} \left[\frac{\text{particles}}{\text{cm}^2\text{-sec-}\frac{\text{MeV}}{\text{nucleon}}} \right] \quad ; \qquad (27)$$

where E is the kinetic energy in MeV/nucleon and M_o is the rest mass energy of a nucleon (938 MeV). However, it has been fairly common in some work to use M_o as 1000 MeV/nucleon in equation (27). The value of N depends on the basic nuclei spectra used, and the value of f is taken from Table 3, Column 5. In this work when protons are treated the value of $f = 1$ and $N = 2.22 \times 10^5$ while for nuclei with $Z > 1$, the value of $N = 3.45 \times 10^4$ and $f \leq 1$ as shown in Table 3. For energies below 1000 MeV/nucleon, the hydrogen and helium spectrum is tabulated numerically and a reasonable attempt is made to preserve the relative abundance ratio of hydrogen to helium (shown in Table 3) for the integral spectrum above 30 MeV/nucleon. For example, the ratio of the N values in equation (27) for the H/He fraction is 6.43 for $E > 1000$ MeV/nucleon, and for energies between 30 and 1000 MeV/nucleon the ratio is 6.05. The net result leads to a ratio above 30 MeV/nucleon of approximate 6.25, which agrees with Table 3. The numerical values of the differential energy spectrum below 1000 MeV/nucleon of hydrogen and helium used in this work is shown in Table 4, and plotted in Figure 4. Above 1 GeV/nucleon, equation (27) is used with the previously defined values of N.

It should be noted that the agreement between measurements and the spectrum used by the writers is not exceptionally good; however, due to the wide scatter in measurements, little else could be done. Therefore, it should be noted that it will be obviously difficult to obtain better-than-rough agreement among different writers unless they resort to the same spectra and relative abundancies. This writer makes no claim to a better set of data; however, the exact spectral data used in the following work are given in Table 4.

TABLE 4. DIFFERENTIAL SPECTRA OF HYDROGEN AND HELIUM $\left[\frac{\text{particles}}{\text{cm}^2\text{-sec-MeV/nucleon}}\right]$

Hydrogen		Helium	
E (MeV)	$J_o(E_A)$	$E_A\left(\frac{\text{MeV}}{\text{nucleon}}\right)$	$J_o(E_A)$
30	4.71(-4)[a]	30	1.11(-4)
50	7.00(-4)	50	2.02(-4)
80	1.01(-3)	80	2.92(-4)
100	1.20(-3)	100	3.28(-4)
150	1.60(-3)	150	3.71(-4)
200	1.83(-3)	200	3.80(-4)
300	2.21(-3)	250	3.75(-4)
350	2.26(-3)	300	3.63(-4)
400	2.27(-3)	350	3.50(-4)
450	2.24(-3)	400	3.36(-4)
500	2.19(-3)	500	3.08(-4)
600	2.02(-3)	600	2.84(-4)
700	1.82(-3)	700	2.63(-4)
850	1.51(-3)	850	2.30(-4)
1000	1.24(-3)	1000	1.92(-4)
For $E \geq 1000$ MeV $J_o(E) = \frac{2.22 \times 10^5}{(1000 + E)^{2.5}}$		For $E \geq 1000$ MeV/nucleon $J_o(E_A) = \frac{3.45 \times 10^4}{(1000 + E_A)^{2.5}}$	

a. The number in parentheses is the power of ten.

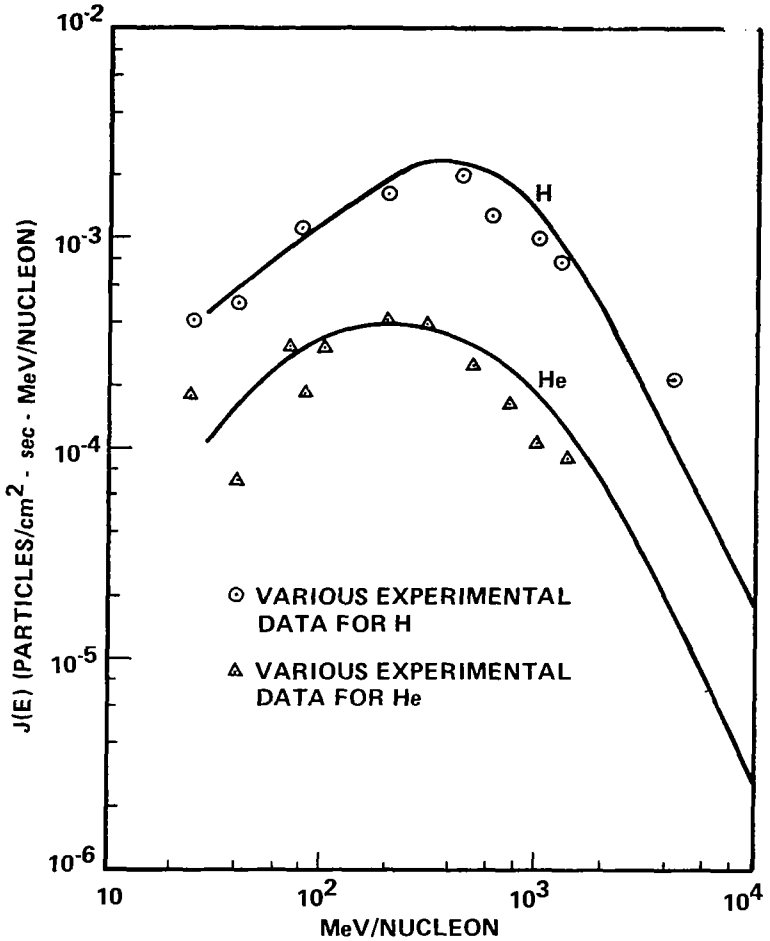

Figure 4. Differential spectra of free space hydrogen and helium nuclei during solar minimum.

SECTION V. FREE SPACE COSMIC RAY DOSE ANALYSIS

Following the methods evolved in the previous sections and using the spectra and relative abundances outlined in Tables 3 and 4, the cosmic-ray dose rates can now be calculated. For reasons of uniformity, the total number of particles above 30 MeV/nucleon will be normalized to 4 particles/cm^2-sec which is the expected value for solar minimum; above about 900 MeV/nucleon the integral spectra is only 2.1 particles/cm^2-sec. The reader may assume with some reservations that all dose rates are simply proportional to the relative number of particles at different times of the solar cycle. However, this is not quite the case since the spectrum shape will be dependent somewhat on the solar cycle.

Thus, based on the above simple correction method, the dose estimates at solar maximum should be somewhat high for thin shields and low for thick shields. For further simplicity, the dose rates have all been tabulated for one year or 3.15×10^7 seconds. Here the correction to shorter time periods should offer no difficulties since the changes in the spectrum should be fairly insensitive to time periods of one year.

The actual dose rates are calculated as follows. The spectrum from Table 4 is numerically extended to contain the point where the energy outside the shield will represent the energy of 900 MeV/nucleon inside the shield which depends on the shield thickness and Z number of the cosmic-ray component in question [see equation (21)]. Above the energy of 900 MeV/nucleon inside the shield the stopping power is assumed to be $2.2\ Z^2$, and the spectrum has the analytical form shown at bottom of Table 4, multiplied by the proper abundancy fraction (f) in Table 3. Following equation (23), the cosmic-ray primary dose equation becomes at depth x and for each Z group:

$$D_p(x) = 1.6 \times 10^{-8}\ f \exp\left[-\Sigma_{in}(A_i)\, x\right] \cdot \left\{ \int_{E_A = \alpha_A^{1/r}}^{E_{max}} J_o(E_A)\, S_x(E^*_A)\, QF(E^*_A)\, dE_A + \frac{2.2\, Z^2\, N \cdot QF\left(\frac{900\,MeV}{nucleon}\right)}{1.5\,(1000 + E_{max})^{1.5}} \right\} \frac{rems}{sec}\ , \tag{28}$$

where $E_{max} = \left[\alpha_A + \beta_A\,(900)^r\right]^{1/r}$; (energy that becomes 900 MeV/nucleon at depth x), and $S_x(E^*_A)$ is defined in equation (24). The $QF(E^*_A)$ is given to depict the more general case and this value is set to 1.00 for calculating the rad doses in tissue. The second term in the bracket represents the integral of equation (27) from E_{max} to infinity.

The value of the integral is obtained by numerical methods since the differential spectrum, $J_o(E_A)$, is taken from the tabulated values described above. The pseudo-total dose is estimated by setting $\Sigma_{in}(A_i) = 0$ in equation (28) [equivalent to equation (26)]. The only undefined term in equation (28) is that of the $\Sigma_{in}(A_i)$ or the inelastic cross section for the target of aluminum ($A_T = 27$) and the incident particle, A_i. For purposes here, the authors have borrowed the approximations of P. H. Aditya [7]. In units of cm^2/g this cross section is given as follows:

$$\text{I. } \Sigma_{in}(A_i) = 2.52 \times 10^{-2} \left(A_i^{1/3} + A_T^{1/3}\right)^2 / A_T \; ; \; Z \geq 3 \tag{29}$$

$$\text{II. } \Sigma_{in}(A_i) = 2.05 \times 10^{-2} \left(4^{1/3} + A_T^{1/3}\right)^2 / A_T \; ; \; Z = 2 \tag{30}$$

$$\text{III. } \Sigma_{in}(A_i) = 1.50 \times 10^{-2} \left(1 + A_T^{1/3}\right)^2 / A_T \; ; \; Z = 1 \tag{31}$$

The values of $\Sigma_{in}(A_i)$ and its reciprocal for $A_T = 27$ are shown in Table 5. The last column is a measure of the mean-free path. The fact that the proton cross section is small may be the author's only excuse for using the approximations suggested in equation (26). Thus one can see that if the above cross sections are approximately correct, then less than 50 percent of all cosmic rays will have suffered a nonelastic collision at 20 g/cm^2 except for the last two nuclei groups $Z = 15$-21 and $Z = 22$-28. At 16 g/cm^2, less than 50 percent of the largest Z group considered will have had nonelastic collisions. For this reason, the writers feel that the approximation given in equation (26) for the estimation of total cosmic-ray doses may be valid up to about 15 g/cm^2, and, for values beyond this thickness, the values tabulated and plotted in this work should be treated with caution. Thus, since the estimation of the secondary dose in thin shields is accomplished here by assuming that the primary dose component removed by a nuclear nucleon collision is equal to the secondary dose, one should feel very insecure when the fictitious secondary dose approaches the true primary doses (this is especially true for protons). Thus, the authors make the following qualifications on this work. Since this paper is devoted to developing approximation methods and their applications, the estimated total cosmic-ray doses and secondary doses presented in the ensuing pages are indicative of a reasonable extrapolation of the authors' methods but should not be construed as necessarily correct.

In any case, the most skeptical reader may feel free to use the presented total-dose rates in rem or rads at 1 or 5 g/cm^2 of aluminum and assume that the added effect of the secondary contribution would be an essentially flat dose rate curve out to about 50 g/cm^2. The less skeptical reader may feel free to use the presented data out to about 15 or 20 g/cm^2. However, the writers have calculated dose values at shield thicknesses of 35 and 50 g/cm^2 for purposes of future comparisons when more accurate methods of secondary dose calculations or measurements are available. It should be noted that some work along this line has been pursued by Curtis and Wilkinson [8]. Their results are not conclusive but they seem to lend validity to the methods used in this report.

Table 6 presents the results of the pseudo-total and primary doses in rads-tissue/year for the 14 nuclei cosmic ray groups (Table 3) using seven aluminum shield thicknesses. The results shown in Table 6 are obtained by using equation (28), as described above. A fictitious secondary dose component is found by subtracting the primary dose from the so-called total dose. It should be noted that for the contribution from all nuclei at 20 g/cm^2,

TABLE 5. VALUES OF INELASTIC CROSS SECTION IN Al^{27}

Avg Z No.	Avg A No.	$\Sigma_{in}\left(\frac{cm^2}{g}\right)$	$1/\Sigma_{in}$
1	1	0.0089	112.51
2	4	0.0160	62.62
4	9	0.0241	41.53
6	12	0.0261	38.30
7	14	0.0273	36.62
8	16	0.0284	35.17
9	19	0.0300	33.36
10	20	0.0305	32.82
11	23	0.0319	31.38
12	24	0.0323	30.95
13	27	0.0336	29.77
14	28	0.0340	29.40
18	37	0.0374	26.72
25	54	0.0429	23.31

the fictitious secondary dose component is only 33 percent. However, for the Z = 25 group one sees that the fictitious secondary contribution is about 58 percent. Thus, when one looks at the pseudo-total rad dose from all components, he should be more secure in using the above approximation methods than when he looks at any group alone.

The summed dose from all nuclei components in the above tables is plotted in Figure 5, along with a comparison to the Z = 25 group. It may be of interest to point out that the calculation of Curtis and Wilkinson [8] gave a total free-space dose of 12.6 rads/year, but they used only five nuclei groups and omitted the heavy nuclei group

TABLE 6. SUMMARY OF CALCULATED COSMIC RAY DOSES IN RADS-TISSUE/YEAR NORMALIZED TO 4 PARTICLES/CM^2-SEC ABOVE 30 MeV/NUCLEON

Pseudo-Total Dose (rads-tissue/year)							
Atomic Group	Shield Thickness – g/cm^2 of Aluminum						
	1	5	10	15	20	35	50
1	4.78	4.73	4.68	4.62	4.57	4.40	4.24
2	3.30	3.24	3.14	3.04	2.96	2.76	2.61
4	0.30	0.29	0.28	0.26	0.25	0.23	0.21
6	1.11	1.03	0.95	0.90	0.85	0.76	0.69
7	0.67	0.61	0.56	0.53	0.50	0.44	0.40
8	1.09	0.98	0.90	0.84	0.80	0.69	0.62
9	0.14	0.13	0.11	0.11	0.10	0.09	0.08
10	0.51	0.45	0.41	0.38	0.36	0.31	0.27
11	0.39	0.35	0.31	0.29	0.27	0.23	0.20
12	0.77	0.67	0.60	0.55	0.52	0.44	0.38
13	0.18	0.15	0.14	0.13	0.12	0.10	0.09
14	0.39	0.34	0.30	0.28	0.26	0.21	0.18
18	0.69	0.58	0.51	0.46	0.43	0.35	0.28
25	2.81	2.31	1.99	1.78	1.61	1.23	0.98
Totals	17.13	15.86	14.88	14.11	13.60	12.24	11.23
Atomic Group	Primary Dose (rads-tissue/year)						
1	4.73	4.53	4.28	4.05	3.82	3.22	2.72
2	3.25	2.99	2.67	2.39	2.15	1.58	1.18
4	0.30	0.26	0.22	0.18	0.16	0.10	0.06
6	1.08	0.90	0.73	0.61	0.51	0.30	0.19
7	0.65	0.53	0.43	0.35	0.29	0.17	0.10
8	1.06	0.85	0.68	0.55	0.45	0.26	0.15
9	0.13	0.11	0.08	0.07	0.06	0.03	0.02
10	0.50	0.39	0.30	0.24	0.19	0.11	0.06
11	0.38	0.30	0.23	0.18	0.14	0.08	0.04
12	0.74	0.57	0.44	0.34	0.27	0.14	0.08
13	0.17	0.13	0.10	0.08	0.06	0.03	0.02
14	0.38	0.29	0.21	0.17	0.13	0.06	0.03
18	0.67	0.48	0.35	0.26	0.20	0.09	0.04
25	2.70	1.86	1.29	0.93	0.68	0.27	0.11
Totals	16.74	14.19	12.01	10.50	9.11	6.44	4.80

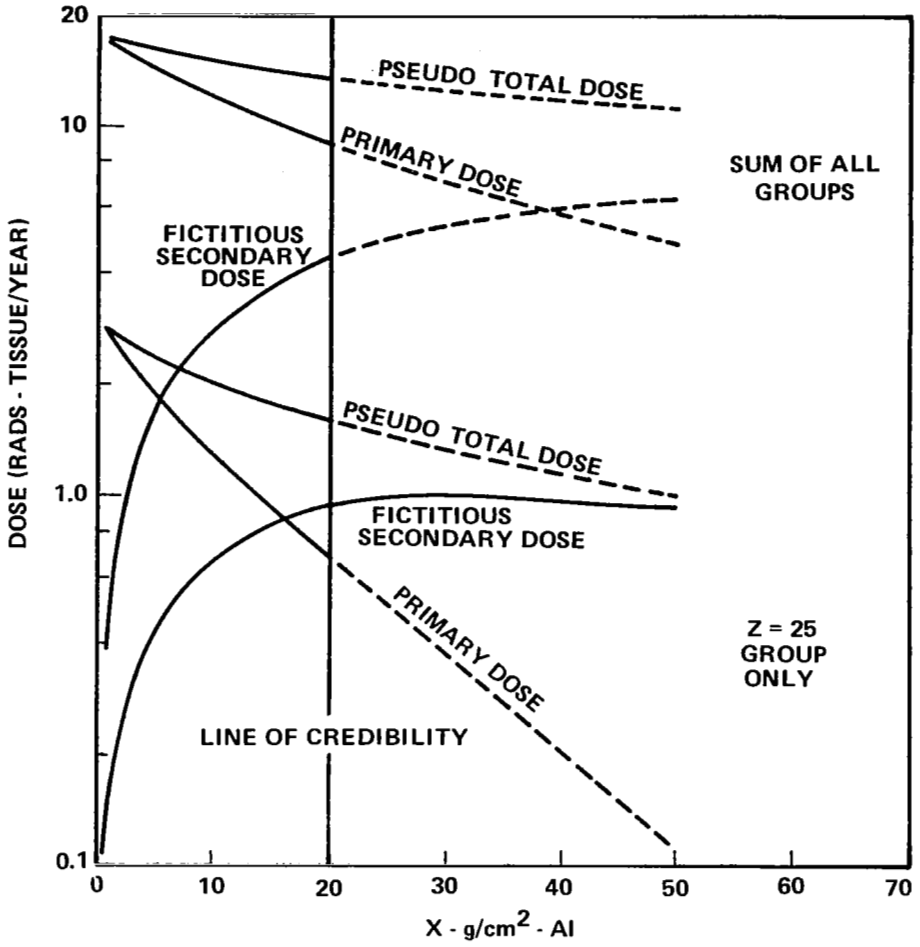

Figure 5. Cosmic ray dose rates in rads as a function of shield thickness.

($15 \leqslant Z \leqslant 25$). However, they used a so-called very heavy group ($26 \leqslant Z \leqslant 28$). In addition it is not clear that their total flux above 30 MeV/nucleon was normalized to 4 particles/cm^2-sec but, perhaps, more nearly to 3.2 particles/cm^2-sec. In which case, our pseudo-total dose behind 1 g/cm^2 (3.2 particles/cm^2-sec) is 13.7 rads-tissue/year which is in fair agreement. The Russians, V. G. Bobkov et al. [9], calculated the unshielded cosmic-ray dose for 2.3 particles/cm^2-sec to be about 8.2 rads-tissue/year. In this case our total dose is about 9.8 rads-tissue/year. However, again the Russian calculation used only five nuclei groups and the above scaling ratio is not quite valid since they used a spectrum for the solar maximum period. As a final check on the above results, it is of interest to make a simple calculation following J. L. Modisette et al. [10] who assumed that the dose rate from the various components is proportional to Z^2 times the relative abundance. However the relative abundance table used by Modisette et al. in Reference 10 is not quite the same as shown in Table 3; hence, a similar table will be made using the presently employed relative abundancies. The results are shown in Table 7. The agreement between the last

TABLE 7. DOSE ESTIMATED BY RELATIVE ABUNDANCIES TIMES Z^2 DEPENDENCE

Element	Relative Abundance	Z^2	Relative Dose	Scaled to 17.13 rads	Rads from Table 6[a]
$_1$H	0.84700	1	0.847	4.96	4.78
$_2$He	0.13550	4	0.542	3.17	3.30
$_3$Li-$_5$B	0.00311	16	0.050	0.29	0.30
$_6$C	0.00508	36	0.183	1.07	1.11
$_7$N	0.00226	49	0.111	0.65	0.67
$_8$O	0.00282	64	0.180	1.05	1.09
$_9$F	0.00028	81	0.023	0.13	0.14
$_{10}$Ne	0.00085	100	0.085	0.50	0.51
$_{11}$Na	0.00054	121	0.065	0.38	0.39
$_{12}$Mg	0.00090	144	0.130	0.76	0.77
$_{13}$Al	0.00017	169	0.029	0.17	0.18
$_{14}$Si	0.00034	196	0.067	0.39	0.39
$_{15}$P-$_{21}$Sc	0.00037	324	0.120	0.70	0.69
$_{22}$Ti-$_{28}$Ni	0.00079	625	0.494	2.89	2.81
Totals	1.00001	——	2.926	17.11	17.13

a. Summed results behind 1 g/cm^2 aluminum.

two columns of Table 7 is very good. The largest absolute disagreement is in the hydrogen and helium components, but it should be recalled that the more accurate methods presented in Table 6 used different spectra for these two components. Thus, it seems that the methods used to calculate the cosmic-ray dose rates for thin shields are not very sensitive to the techniques employed, as long as the correct units, magnitudes, and relative abundances are known. This is important to know since most spacecraft have relatively thin walls and

TABLE 8. SUMMARY OF CALCULATED COSMIC RAY DOSES IN REM/YEAR NORMALIZED TO 4 PARTICLES/CM^2-SEC ABOVE 30 MeV/NUCLEON

Psuedo-Total Dose (rem/year)								
Atomic No. Group	Shield Thickness – g/cm^2 of Aluminum							Q.F. at x = 10 g/cm^2
	1	5	10	15	20	35	50	
1	4.06	4.01	3.96	3.91	3.86	3.71	3.58	0.85
2	3.68	3.60	3.43	3.29	3.17	2.91	2.72	1.09
4	0.65	0.59	0.54	0.50	0.47	0.42	0.38	1.93
6	4.02	3.50	3.08	2.81	2.61	2.23	1.97	3.24
7	3.02	2.57	2.25	2.04	1.88	1.59	1.41	4.02
8	5.97	4.99	4.33	3.91	3.60	3.02	2.66	4.81
9	0.89	0.75	0.65	0.59	0.54	0.45	0.40	5.91
10	3.77	3.16	2.73	2.45	2.25	1.87	1.63	6.66
11	3.28	2.74	2.37	2.14	1.98	1.64	1.42	7.65
12	7.16	5.91	5.10	4.59	4.22	3.49	3.00	8.50
13	1.83	1.51	1.31	1.18	1.08	0.89	0.77	9.36
14	4.43	3.64	3.14	2.83	2.59	2.12	1.78	10.47
18	9.86	8.03	6.89	6.17	5.64	4.52	3.66	13.51
25	51.95	42.13	36.07	32.09	29.02	22.02	17.45	18.13
Totals	104.57	87.13	75.85	68.50	62.91	50.88	42.83	
Avg. Q.F.	6.10	5.49	5.10	4.85	4.63	4.16	3.81	
Atomic Group	Primary Dose (rem/year)							
1	4.03	3.84	3.62	3.42	3.23	2.72	2.29	
2	3.63	3.32	2.92	2.59	2.31	1.66	1.22	
4	0.63	0.53	0.43	0.35	0.29	0.18	0.11	
6	3.92	3.07	2.37	1.90	1.55	0.89	0.54	
7	2.94	2.24	1.71	1.35	1.09	0.61	0.36	
8	5.80	4.33	3.26	2.55	2.04	1.12	0.64	
9	0.86	0.65	0.48	0.37	0.30	0.16	0.09	
10	3.66	2.72	2.01	1.55	1.22	0.64	0.35	
11	3.18	2.33	1.73	1.33	1.05	0.54	0.29	
12	6.93	5.03	3.69	2.83	2.21	1.13	0.60	
13	1.77	1.28	0.93	0.71	0.55	0.28	0.14	
14	4.28	3.07	2.24	1.70	1.31	0.65	0.32	
18	9.50	6.66	4.74	3.52	2.67	1.22	0.56	
25	49.77	34.00	23.49	16.86	12.30	4.91	2.04	
Total	100.90	73.07	53.62	41.03	32.12	16.71	9.55	

the unknown secondary contribution, hopefully, will not lead to large uncertainties. In fact, a common approach is simply to assume that the cosmic-ray dose rate remains constant through the shield and the astronaut. This approach could not be very far astray since the pseudo-total rads-tissue dose in Table 6 shows that the total rad dose at 15 g/cm^2 is about 82 percent of the 1 g/cm^2 dose, and at 35 g/cm^2 the dose is still 71.5 percent of the 1 g/cm^2 dose.

The foregoing is useful but perhaps the most desired dose rates for effects on man are the rem/year calculations which are shown in Table 8 for the pseudo-total and primary rem doses. For additional information, Table 8 has a row labeled "average quality factor" which was obtained by dividing the summed rem dose of Table 8 by the summed rad dose of Table 6. This value should be an indicator of a reasonable average quality factor to use for cosmic rays. Also the last column of Table 8 contains the quality factor for each cosmic-ray component behind 10 g/cm^2 of shield. It should be noted that the rem dose for the hydrogen component is less than the corresponding rad dose. This follows from the use of equation (8) which permits a minimum quality factor of about 0.82 for protons above 900 MeV in tissue. The total rem/year dose from protons is probably not valid since the secondary particle's rem dose is not correct.

TABLE 9. COSMIC RAY DOSE RATES FROM V. G. BOBKOV ET AL.
[2.3 PARTICLES/CM^2-SEC]

			From V. G. Bobkov et al.[a]				From Tables 6 & 8[b] Scaled to 2.3 part./cm^2-sec		
Nuclei Group	Z Group	$\bar{A}$	Relative Abundance	Rads/ Year	Rem/ Year	QF	Rads/ Year	Rem/ Year	QF
P	1	1	0.8515	2.26	2.26	1.00	2.75	2.33	0.85
He	2	4	0.1320	1.35	1.35	1.00	1.90	2.11	1.11
L	3-5	10	0.0020						
M	6-9	14	0.0102	1.24	4.05	3.3	1.73	7.99	4.62
H	10-20	31	0.0034	1.83	12.41	6.8	1.68	17.44	10.35
VH	> 20	51	0.0009	1.50	26.50	17.7	1.61	29.87	18.48
	Totals		1.0000	8.18	46.57	5.7	9.67	59.74	6.10

a. Free space dose

b. Behind 1 g/cm^2 of aluminum

To make some type of comparison to the results shown in Table 8, the results of V. G. Bobkev et al. [9] are summarized in Table 9. However they used only five nuclei groups and their spectrum is for solar maximum. In this report, an attempt has been made to group data according to Bobkov by using the VH group as the authors' Z = 25 group (22-28) and to obtain the H group by summing all components from Z = 10 through Z = 21. In general, the agreement is fair, considering the simplifications made.

In Figures 6 and 7 the data of Table 8 are plotted. It should be noted that the Z = 25 group (Fig. 7) represents approximately 50 percent of the total rem dose. This fact indicates the necessity for obtaining accurate data for the Z = 20-30 nuclei range and the importance of correctly defining a quality factor for the VH cosmic radiation component. Here a quality factor of about 18 has been derived which agrees with the Russian work.

To evaluate the credibility of the foregoing cosmic-ray dose rates as a function of depth, the results of V. G. Bobkov et al. for solar maximum, are compared against the present calculations. The results are shown in Figure 8. Considering the spectral differences, the agreement is probably good; however, their secondary dose calculation methods seem to be no improvement over those used in this report. In the case of the rem/year dose, the agreement is not as good, but it is well worth noting that from about 30 g/cm^2 to 50 g/cm^2 the rem dose curves are essentially parallel even though our numbers are about 20 to 25 percent lower. However, the doses calculated here should be higher for thin shields and lower for thick shields since the integral flux above about 900 MeV/nucleon is probably lower than that of Bobkov et al., after the ratio of 2.3/4 is applied over the total spectrum. Another source of disagreement between the rem/year doses could be the quality factors used. Bobkov et al. probably derived a more constant quality factor as a function of shield thickness since their low energy component was smaller than the values obtained here. Thus, in Table 8 a quality factor of 6.1 is found behind 1 g/cm^2 and of 3.81 behind 50 g/cm^2. If the quality factor at 50 g/cm^2 was 5, then the authors' dose results in rem/year would agree with Bobkov at 50 g/cm^2.

It should be pointed out that the proper quality factors to use for heavy particles are in wide disagreement [3]. In this study no attempt is made to evaluate the effects of microbeam tracks from single events.

SECTION VI. CALCULATION OF COSMIC RAY DOSE RATES FOR EARTH ORBITAL MISSIONS

In the previous sections of this report the effort has been limited to evaluation of the cosmic-ray dose rates in free space or outside the earth's magnetic field. However, many future space missions of interest are essentially circular orbits inside the earth's magnetic field. The major problem in attempting to define galactic cosmic-ray dose rates is determining the average intercepted differential spectrum over a period of at least one week. The

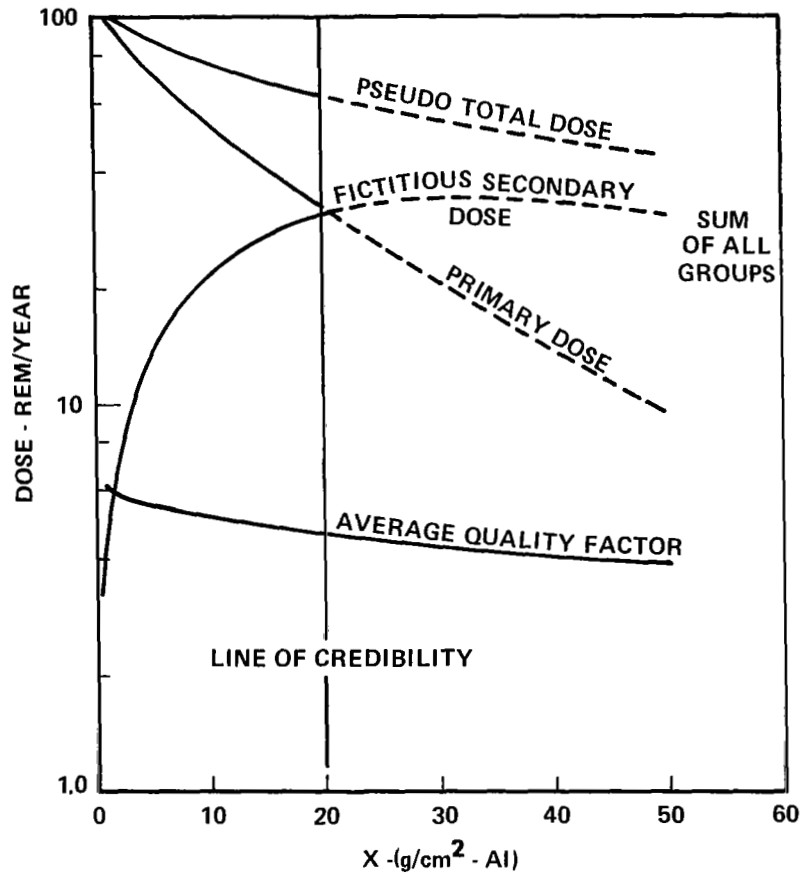

Figure 6. Cosmic ray dose rates in rems as a function of shield thickness.

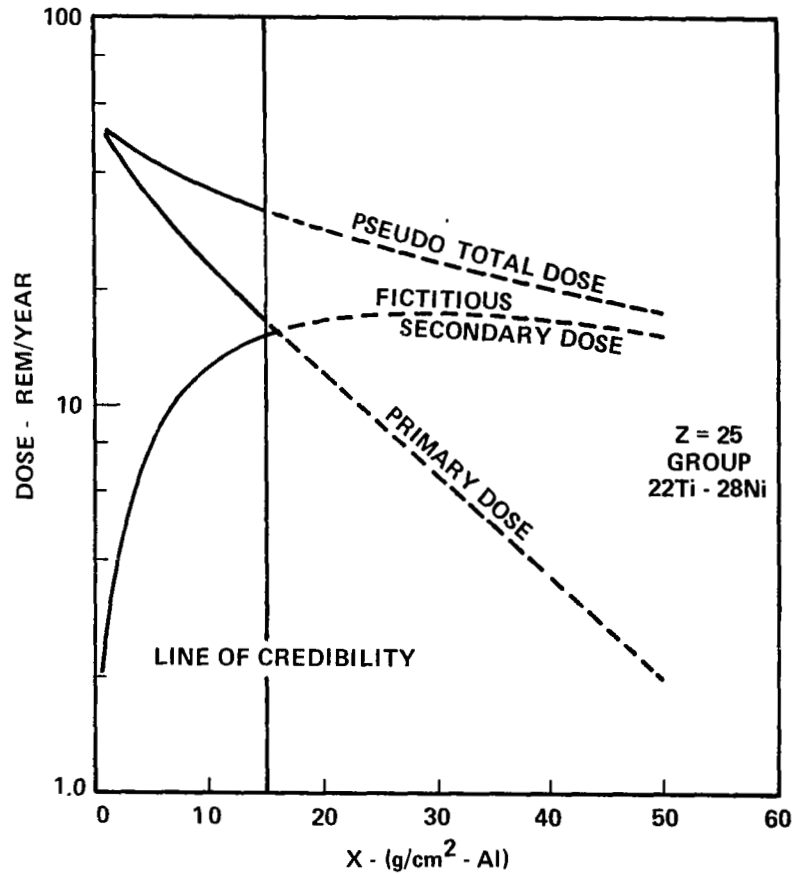

Figure 7. Cosmic ray dose rates in rems for very heavy nuclei.

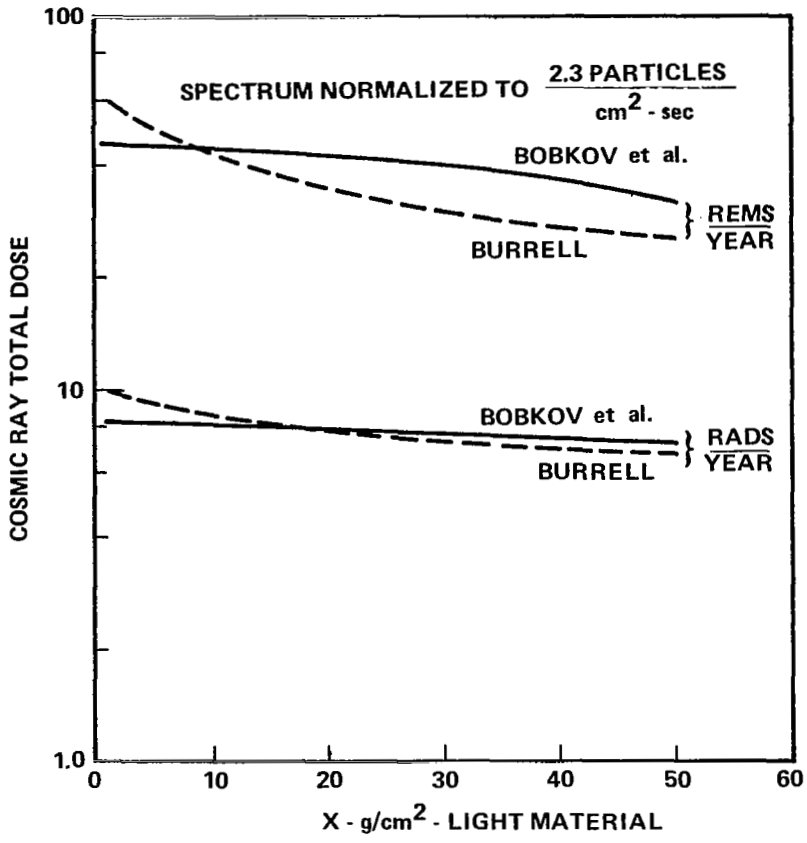

Figure 8. Comparison of cosmic ray dose rates as a function of shield thickness.

major uncertainty in these calculations is the rather complex magnetic field of the earth and the simplifying assumption of an eccentric dipole field for the earth in order to obtain a tractable problem. The following development by J. J. Wright[1] is an attempt to arrive at useful methods for approximating the cosmic-ray spectrum in circular earth orbits where the spectrum will be average over several days flight.

The magnetic field of the earth acts as a rigidity analyzer on the free space cosmic ray spectrum. Restrictions are placed on the motion of the particles to allow particles having a ridigity equal to or greater than a minimum value to reach a particular position. From Störmer's work [11] the rigidity is given by

$$P_C = \frac{59.9 \cos^4 \lambda}{R^2 \left\{ 1 + (1 - \sin \epsilon \cos \Upsilon \cos^3 \lambda)^{1/2} \right\}^2} \qquad (32)$$

1. NASA TN to be published in 1971.

where λ is the geomagnetic latitude, ϵ the zenith angle ($\epsilon = 90°$ in this study), R the radial distance from the dipole center (Re units), Υ the azimuth angle of the Störmer cone measured from the east and P_c is the magnetic rigidity (GV units).

The cutoff momentum for a dipole field is given by

$$P = P_c Z/c \quad . \tag{33}$$

If $P \times c$ is in electron volts, then P_c is in volts, where Z in the number of electron charge units. Combining equations (32) and (33), the particle momentum is given by

$$P\left[\frac{GeV}{c}\right] = \frac{59.9\, Z \cos^4 \lambda}{R^2 \left\{1 + (1 - \cos \Upsilon \cos^3 \lambda)^{1/2}\right\}^2} \quad . \tag{34}$$

The Störmer cone is closed, giving the minimum momentum needed to arrive at the position (P_{min}), when $\Upsilon = 180°$ or

$$P_{min} = \frac{59.9\, Z \cos^4 \lambda}{R^2 \left[1 + (1 + \cos^3 \lambda)^{1/2}\right]^2} \quad . \tag{35}$$

The allowed cone is completely open when $\Upsilon = 0°$ or

$$P_{max} = \frac{59.9\, Z \cos^4 \lambda}{R^2 \left[1 + (1 - \cos^3 \lambda)^{1/2}\right]^2} \quad . \tag{36}$$

The energy is obtained through the relativistic equation

$$T = \left[P^2 c^2 + m_o^2 c^4\right]^{1/2} = E + m_o c^2 \quad , \tag{37}$$

where T is the total energy (per nucleon), E is the kinetic energy per nucleon, and $m_o C^2$ is the rest mass energy of a nucleon. From equation (37), the kinetic energy is represented by

$$E = \left[\left(\frac{Z}{A}\right)^2 P_c^2 + m_o^2 c^4\right]^{1/2} - m_o c^2 \quad . \tag{38}$$

The charge-to-mass ratio (Z/A) is 1 for singly charged particles and ~ 1/2 for heavier particles. When equation (38) is substituted into equation (34), one obtains the azimuth angle of the allowed cone as a function of position in space and particle kinetic energy. From the azimuth angle one can determine the ratio of the solid angle of the allowed cone to the total solid angle giving the fraction of the free-space particles of kinetic energy E reaching the position in space. This fraction times the free-space spectrum gives the modified spectrum at energy E.

The computer program which has been developed calculates the time-weighted modified-energy spectrum of primary cosmic rays and solar cosmic radiation on any feasible earth orbit by varying the angle over the allowed cone from the value of equation (35) to the value given by equation (36) or from $\Upsilon = 180$ deg to $\Upsilon = 0$ deg. At each position in orbit the modified spectrum is also weighted by the time interval at each position of the orbit.

The geomagnetic field is represented by an eccentirc dipole. The dipole is translated 0.0685 Re (earth radii) from the geographic center and tilted 11.7 deg from the geographic pole. Using this model one obtains the geomagnetic latitude λ used in equation (32). These calculations incorporate the shadow effect of the solid earth, ignoring the atmosphere and its albedo. The modified energy spectra are averaged over several days and then used to calculate the dose rates behind various shield thicknesses of a spacecraft.

Figures 9 and 10 show results, using the above methods, for the averaged proton and alpha spectra of Table 4 in a 463-km (250-n.mi.) circular orbit for various inclinations from 0 to 90 deg compared to the free-space spectrum. The above spectra reflect the solid angle subtended by the earth at 463 km which is approximately 32 percent of the 4π space. Hence, the high-energy spectrum tail for the various orbits does not approach the free-space spectra but approaches only 68 percent of the free-space, high-energy tail as shown in Figures 9 and 10.

Using the spectra in Figures 9 and 10, the dose rate in rads-tissue/year and rem/year are calculated in the same manner as described in the preceding section. However, because of the large amount of data obtained in our calculations, the following condensation and depletion of data will be made for the orbital cosmic-ray dose rates. Only the pseudo-total dose rates will be shown in rads and rems; thus, the primary particle dose rates are omitted. Since the number of nuclei groups are so large in Tables 6 and 8 the results will be summarized into the nuclei groups shown in Table 10. However, in using the results summarized (Table 10), it should be understood that all the nuclei groups of Table 3 were used individually for calculation of dose rates and summed merely for the group totals depicted. For additional brevity of tables only shield thicknesses of 1, 5, 10, and 20 g/cm^2-Al will be presented. This is in keeping with the range of penetration depths which is believed to be tenable when using the approximation methods of the previous section. Using the spectra of Figures 9 and 10, the pseudo-total dose rate in rads/year and rems/year for 463-km circular orbits at various inclinations are summarized in Tables 11 and 12.

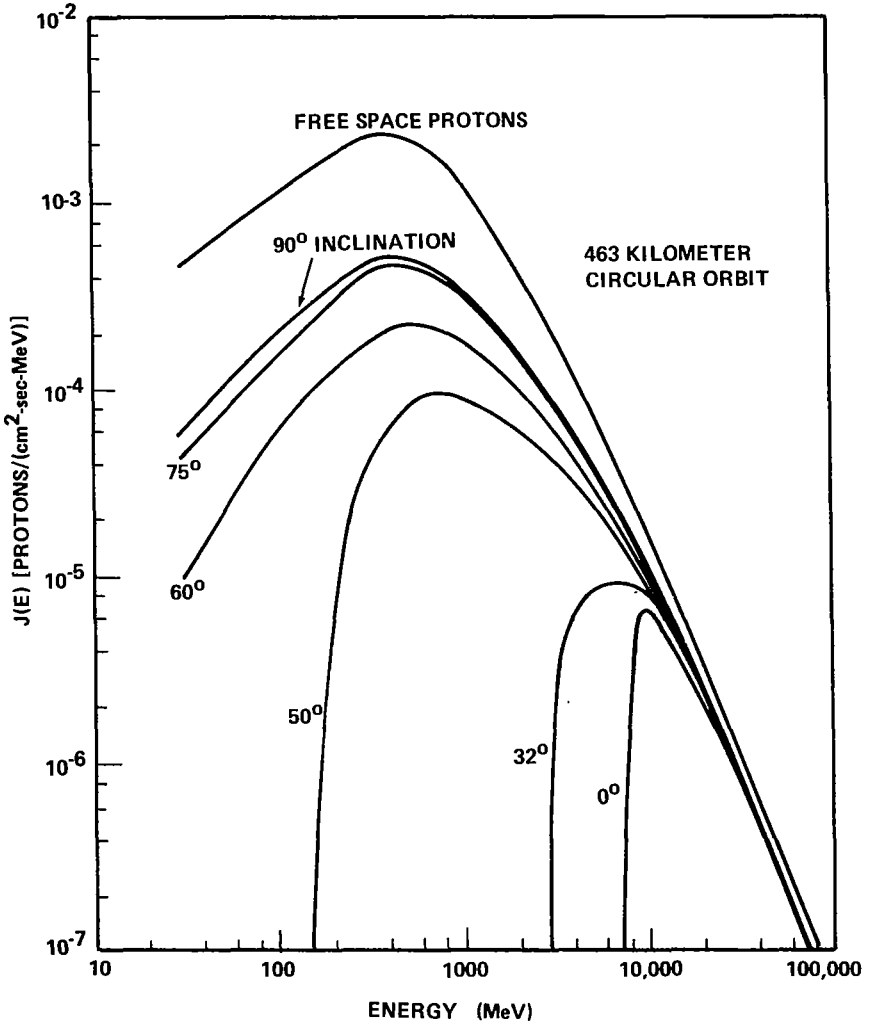

Figure 9. Differential energy spectra for protons in a 463-km orbit.

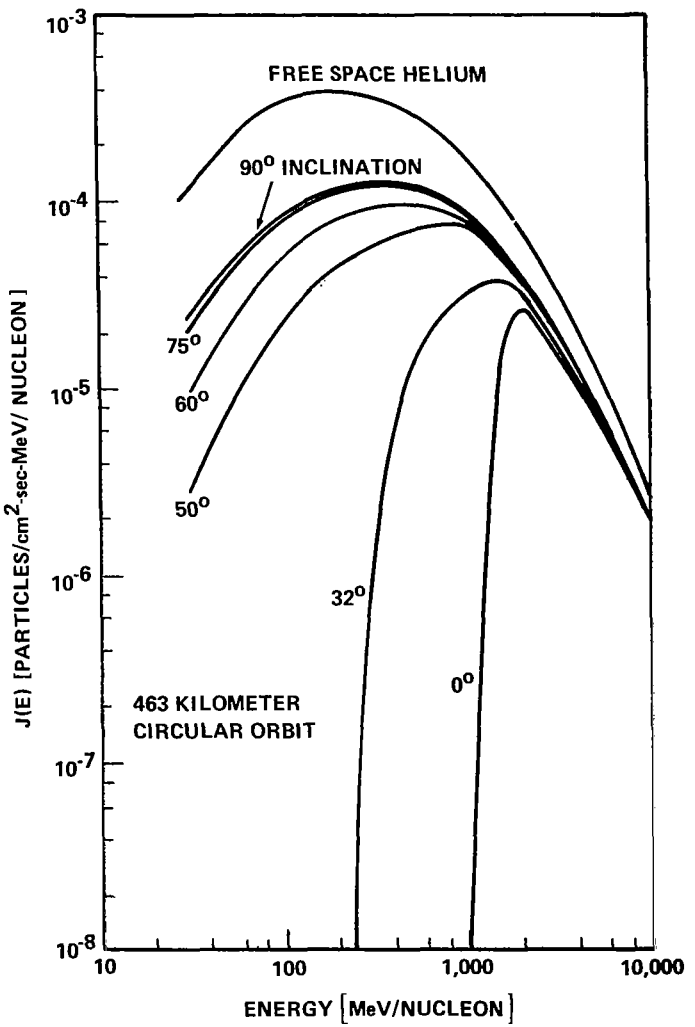

Figure 10. Differential energy spectra for helium nuclei in a 463-km orbit.

TABLE 10. NUCLEI GROUPS FOR ORBITAL CALCULATIONS

Group Name	Z Range	A Range	Rel. Abundance
P	1	1	0.84700
α	2	4	0.13550
L+M	3-9	6-19	0.01355
H	10-21	20-45	0.00317
VH	22-28	48-59	0.00079
———	———	Total	1.00001

The results of Tables 11 and 12 are plotted in Figures 11 and 12 as a function of orbital inclination for the indicated shield thicknesses. The curves shown in Figures 11 and 12 are similar in appearance to cosmic-ray flux or dose data as a function of geomagnetic latitude. However there are basic differences since the spectra used in Figures 9 and 10 reflect the impact of an orbit which necessarily passes over the magnetic equator twice with each revolution, consequently depleting the protons more severely than the heavier nuclei. The results of Tables 11 and 12 indicate that, except for orbits with inclinations greater than 50 deg, the shielding has little or no effect out to 20 g/cm^2. Also, the proton component of the dose is a small fraction of the total dose which reduces the importance of their secondaries.

The effects of using very hard spectra are clearly demonstrated in Table 12 for the 32-deg inclination orbits. If the spectra of Figure 10 are examined with the dose results of the 32-deg inclination orbit in mind, one can see the impact of the increasing stopping power from the degraded energy on the rem/year dose which increases in value out to 20 g/cm^2. Similar results are often shown by other authors for depth-dose calculation when using a free-space environment. Usually, the implication is that the dose increase is due entirely to secondary particle buildup, but, if the spectrum is carefully examined, it often seems to be similar to the hardened spectra shown in Figures 9 and 10. A second factor that contributes to other writers' depiction of an increasing dose rate as a function of shield thickness is their great attendance to the proton secondaries while ignoring the very high ionization rates of the very small percent of heavy nuclei. It is believed that the present paper will tend to clarify some of these points by demonstrating the dramatic effect of the heavy ions on the total cosmic-ray dose rates. For example, at the 50-deg inclination orbit of Table 11, the proton rad/year dose component is only about 10 percent of the summed total dose behind 1 g/cm^2 shield; while the corresponding rem/year dose

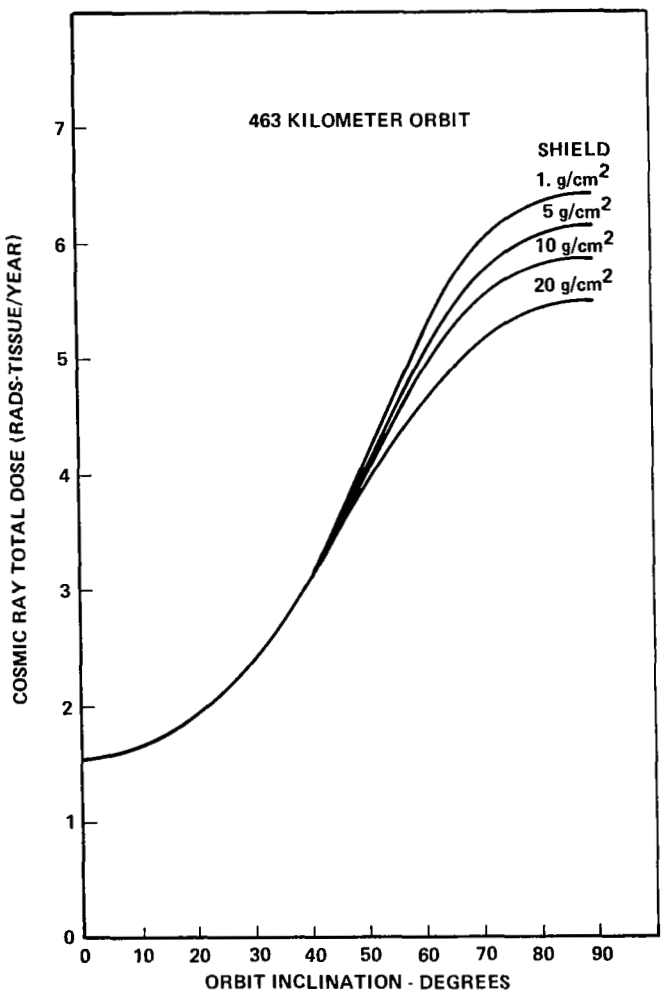

Figure 11. Cosmic-ray dose rates in rads in a 463-km orbit as a function of orbit inclination and shield thickness.

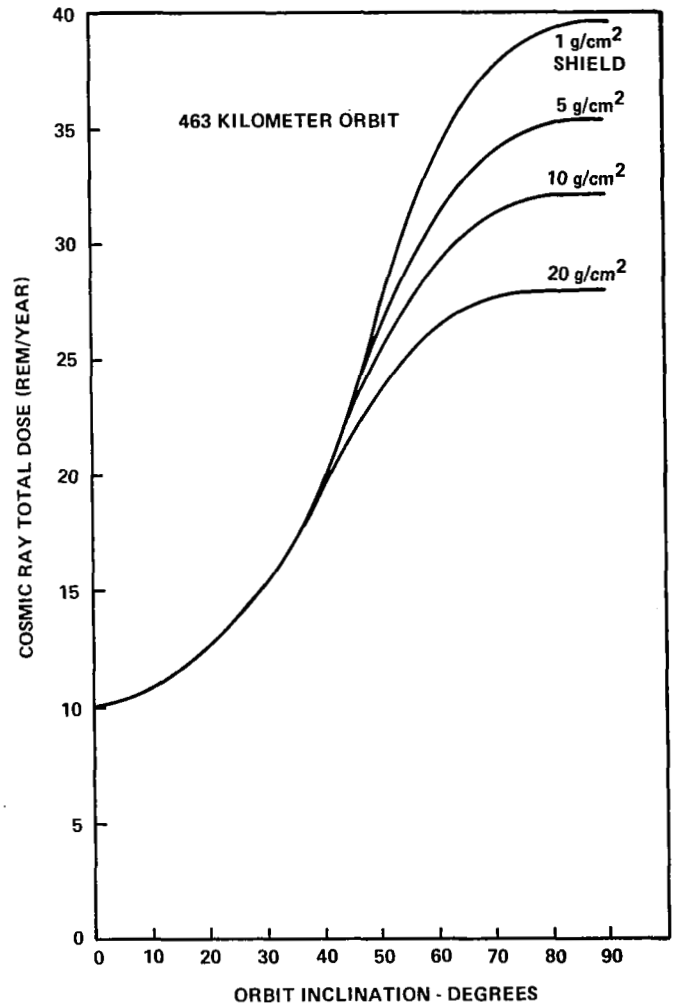

Figure 12. Cosmic-ray dose rates in rems in a 463-km orbit as a function of orbit inclination and shield thickness.

TABLE 11. SUMMARY OF COSMIC-RAY PSEUDO-TOTAL DOSES IN RADS-TISSUE/YEAR[a] FOR 463-km CIRCULAR ORBITS

Nuclei Group	0 deg Inclination, Shield Thickness – g/cm²-Al				32 deg Inclination, Shield Thickness – g/cm²-Al			
	1	5	10	20	1	5	10	20
P	0.08	0.08	0.08	0.08	0.15	0.15	0.15	0.15
α	0.37	0.37	0.37	0.37	0.59	0.59	0.59	0.59
L+M	0.38	0.38	0.38	0.38	0.60	0.60	0.60	0.60
H	0.35	0.35	0.35	0.35	0.53	0.53	0.53	0.53
VH	0.34	0.34	0.34	0.34	0.53	0.54	0.54	0.53
Totals	1.52	1.52	1.52	1.52	2.40	2.41	2.41	2.40
	50 deg Inclination				60 deg Inclination			
P	0.44	0.44	0.44	0.45	0.75	0.75	0.76	0.75
α	0.97	0.98	0.97	0.97	1.16	1.16	1.15	1.14
L+M	0.98	0.98	0.97	0.95	1.18	1.16	1.13	1.05
H	0.88	0.88	0.84	0.81	1.05	1.03	0.96	0.88
VH	0.88	0.85	0.81	0.74	1.04	0.97	0.90	0.79
Totals	4.15	4.13	4.03	3.92	5.18	5.07	4.90	4.61
	75 deg Inclination				90 deg Inclination			
P	1.17	1.17	1.17	1.16	1.26	1.26	1.25	1.24
α	1.34	1.33	1.31	1.27	1.36	1.36	1.33	1.29
L+M	1.34	1.28	1.24	1.15	1.38	1.31	1.25	1.18
H	1.20	1.12	1.05	0.95	1.22	1.14	1.05	0.96
VH	1.18	1.05	0.96	0.83	1.20	1.07	0.97	0.83
Totals	6.23	5.95	5.73	5.36	6.42	6.14	5.85	5.50

a. Primary dose plus fictitious secondary dose at solar minimum.

TABLE 12. SUMMARY OF COSMIC RAY PSEUDO-TOTAL DOSES[a] IN REM/YEAR FOR 463-km CIRCULAR ORBITS

Nuclei Group	0 deg Inclination				32 deg Inclination			
	Shield Thickness – g/cm^2-Al				Shield Thickness – g/cm^2-Al			
	1	5	10	20	1	5	10	20
P	0.07	0.07	0.07	0.07	0.12	0.12	0.12	0.12
α	0.35	0.35	0.35	0.35	0.55	0.56	0.56	0.56
L+M	1.14	1.14	1.14	1.14	1.80	1.81	1.81	1.85
H	2.48	2.49	2.49	2.49	3.69	3.71	3.78	3.85
VH	5.85	5.86	5.85	5.85	9.23	9.35	9.45	9.37
Totals	9.89	9.91	9.90	9.90	15.39	15.55	15.72	15.75
	50 deg Inclination				60 deg Inclination			
P	0.37	0.37	0.37	0.37	0.62	0.63	0.63	0.63
α	0.95	0.96	0.96	0.95	1.16	1.17	1.16	1.14
L+M	2.92	2.93	2.88	2.77	3.85	3.75	3.58	3.32
H	7.13	7.02	6.76	6.35	9.07	8.62	8.06	7.22
VH	15.69	15.10	14.40	13.25	17.81	16.43	15.06	13.99
Totals	27.06	26.38	25.37	23.69	32.51	30.60	28.49	26.30
	75 deg Inclination				90 deg Inclination			
P	0.97	0.97	0.97	0.96	1.06	1.05	1.05	1.03
α	1.38	1.37	1.35	1.29	1.42	1.41	1.37	1.32
L+M	4.82	4.45	4.12	3.70	4.98	4.59	4.22	3.76
H	10.93	9.82	8.92	7.81	11.24	10.02	9.09	7.94
VH	20.43	18.02	16.22	14.05	20.86	18.31	16.43	14.07
Totals	38.53	34.63	31.58	27.81	39.56	35.36	32.16	28.12

a. Primary dose plus fictitious secondary dose at solar minimum.

in Table 12 shows that protons constitute only 1.4 percent of the total rem dose. This implies that large errors in the proton secondary dose will not affect the answers greatly.

Two more altitudes are evaluated in this section for earth-orbit missions at 3189 km (1/2 earth radius) and 6378 km (1 earth radius). Further abbreviations of data are made since only 0, 32, 60, and 90 deg inclinations are considered and dose rates are given behind only one shield thickness of 1 g/cm^2 of aluminum. Table 13 summarizes the above calculations in rads/year and rems/year dose units. Figures 13, 14, and 15 depict the data shown in Table 13.

SECTION VII. CONCLUSIONS

The preceding sections have described approximation methods for treating the transport of cosmic-ray nuclei and the associated dose rates. The methods used to treat secondary and fragmentation particles are superficial at best. At the present level of theory and technique, it is believed that a fairly adequate calculation could be made for the secondary dose components of protons, and probably helium nuclei [12]. However, this was not attempted in the present study for two major reasons. The first is that the computational effort is very extensive, and the second is that for thin shields the main rem dose contributors are the heavy nuclei. Even if the rem dose rates for protons and helium are low by a factor of two, the total dose is affected only a few percent, as can be seen in Tables 8 and 12.

It is the belief of the present writers that this study should place the galactic cosmic-ray dose rates in their proper perspective as a hazard to spaceflight. The assumption has usually been that during solar minimum the galactic cosmic-ray dose was only about 13 rads/year, and that the rem dose was about the same. The quality factor was arbitrarily set at 1.0, since so little is known about the biological damage of heavy nuclei. If the rem dose results presented in this report are meaningful, then the annual dose behind a thin shield may well be close to 100 rem/year during solar minimum and perhaps 50 rem/year during solar maximum. From the above conclusions it is seen that galactic cosmic rays may be a more formidable risk to extended space missions than the solar protons associated with large flares. For example, during the very active 19th solar cycle, the total point detector dose from all solar protons behind 10 g/cm^2 of aluminum was less than 300 rems during the total 6 years of major activity [13]. During a 6-year solar minimum period, the galactic cosmic-ray dose would have been about double the above solar proton rem dose and would have been equal in value during the same period if rem units are used. Furthermore, the solar proton particles are more easily shielded. If the shield is increased from 10 g/cm^2 to about 15 g/cm^2, the solar-proton dose is reduced by more than a factor of two, whereas the reduction in the cosmic ray dose is only a few percent. The major argument for the great concern for solar flare protons is that a large dose may be received during a

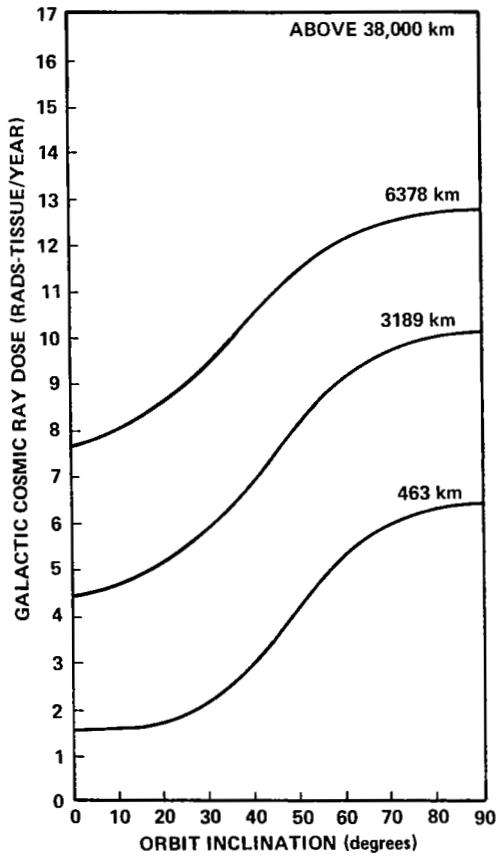

Figure 13. Cosmic-ray dose rates in rads as a function of orbit altitude and inclination

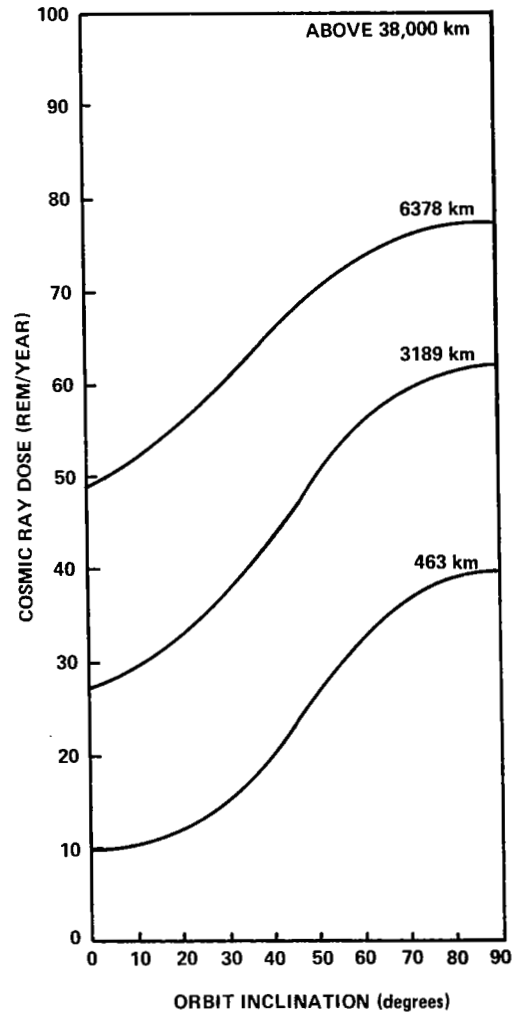

Figure 14. Cosmic-ray dose rates in rems as a function of orbit altitude and inclination.

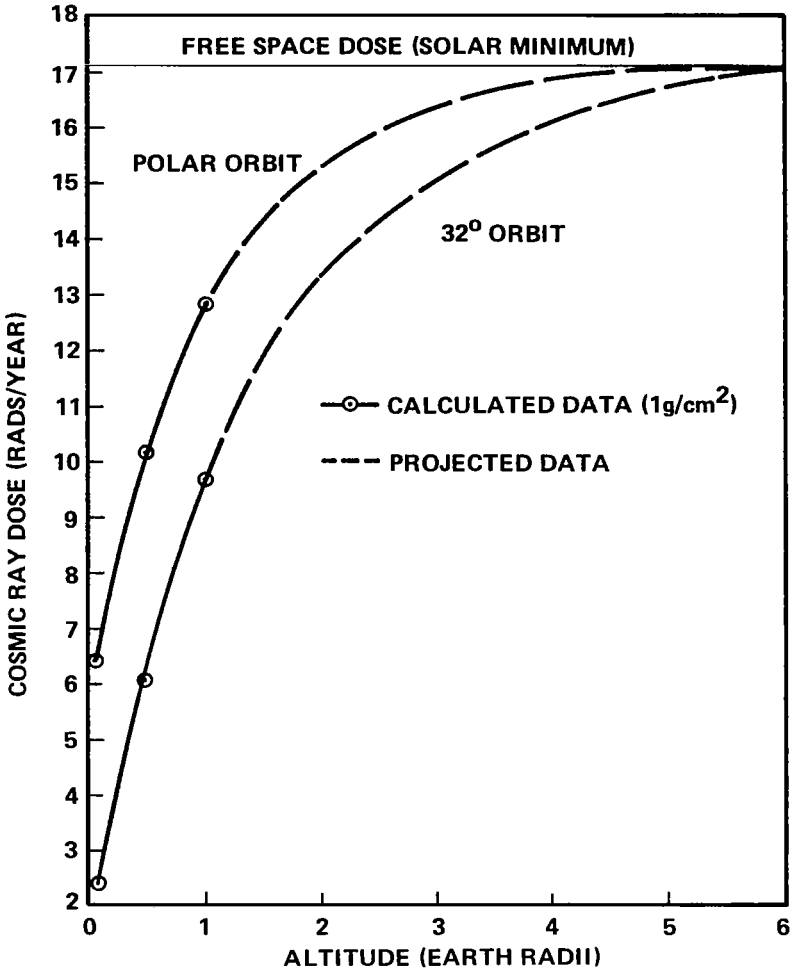

Figure 15. Cosmic-ray dose rates in rads as a function of orbit altitude for two inclinations.

short period of only a week. However, if the events of the extreme 19th cycle are examined, it is found that only about one third of the total 6-year dose (100 rem) was the maximum dose received during a single year [13]. Thus, for missions which last at least one year, the cosmic-ray dose is at least of equal importance and much more difficult to shield against.

TABLE 13. SUMMARY OF COSMIC RAY PSEUDO-TOTAL DOSE RATES BEHIND 1 g/cm² SHIELD FOR CIRCULAR ORBITS AT HIGH ALTITUDES

Inclination of Orbit	Orbit Altitude = 0.5 R_e = 3189 km							
	0 deg		32 deg		60 deg		90 deg	
Nuclei Group	Rad/ Year	Rem/ Year	Rad/ Year	Rem/ Year	Rad/ Year	Rem/ Year	Rad/ Year	Rem/ Year
P	0.26	0.22	0.50	0.42	1.42	1.17	1.95	1.63
α	1.07	1.02	1.44	1.38	2.02	2.08	2.17	2.27
L+M	1.09	3.36	1.46	4.40	2.06	6.86	2.18	7.73
H	0.98	6.90	1.33	9.32	1.85	15.56	1.96	17.10
VH	0.97	16.50	1.32	22.60	1.81	31.11	1.91	33.07
Totals	4.37	28.00	6.05	38.10	9.16	56.78	10.17	61.80

Inclination of Orbit	Orbit Altitude = 1.0 R_e = 6378 km							
	0 deg		32 deg		60 deg		90 deg	
Nuclei Group	Rad/ Year	Rem/ Year	Rad/ Year	Rem/ Year	Rad/ Year	Rem/ Year	Rad/ Year	Rem/ Year
P	0.60	0.51	1.12	0.94	2.31	1.94	2.72	2.30
α	1.83	1.77	2.20	2.18	2.58	2.72	2.66	2.83
L+M	1.86	5.63	2.24	6.98	2.61	8.85	2.68	9.34
H	1.69	12.05	2.04	14.61	2.34	19.14	2.40	19.90
VH	1.68	29.38	2.04	36.43	2.30	41.62	2.34	42.44
Totals	7.66	49.34	9.64	61.14	12.14	74.27	12.80	76.81

Altitude Above 6.0 R_e		
Nuclei Group	Rad/ Year	Rem/ Year
P	4.78	4.06
α	3.30	3.68
L+M	3.31	14.55
H	2.93	30.33
VH	2.81	51.95
Totals	17.13	104.57

REFERENCES

1. Reetz, Art, Ed.: Second Symposium on Protection Against Radiation in Space, NASA SP-71, 1964, pp. 493-505.

2. Burrell, M. O.: The Calculation of Proton Penetration and Dose Rates, NASA TM X-53063; 1964.

3. Langham, Wright H., Ed.: Radiobiological Factors in Manned Space Flight, National Academy of Sciences, Pub. No. 1487, 1967.

4. Hill, C. W., et al.: Data Compilation and Evaluation of Space Shielding Problems, Volume I, Range and Stopping Power Data, Lockheed Engineering Report-7777, 1965.

5. Biswas, S. and Fichtel, C. E.: Nuclear Composition and Rigidity Spectra of Solar Cosmic Rays, Astrophys. J. 139, 941-50, 1964.

6. Charakhchyan, A. N. and T. N.: International Conference on Cosmic Rays, Jaipur Proceedings, Vol. 3., December 1963, pp. 384-389.

7. Aditya, P. H.: Proceedings International Conference on Cosmic Rays, Jaipur, Vol. 5, 1964, p. 64.

8. Curtis, S. B. and Wilkinson, M. G.: Study of Radiation Hazards to Man on Extended Missions, NASA CR-1037, May 1968.

9. Bobkov, V. G., et al.: Radiation Safety During Space Flight. NASA Technical Translation, NASA TT F-356, May 1966, p. 59.

10. Modisette, Jerry J., et al.: from Protection Against Space Radiation, NASA SP-169 1968, p. 4.

11. Störmer, C.: The Polar Aurora, Oxford University Press, London and New York, 1955.

12. Alsmiller, R. G., Jr.: High-Energy Nucleon Transport and Space Vehicle Shielding, Nucler Science and Engineering, Vol. 27 (1967).

13. Burrell, M. O.: The Risk of Solar Proton Events to Space Missions, NASA TN D-6379, June 1971, p. 7.

NASA-Langley, 1972 — 4 M444